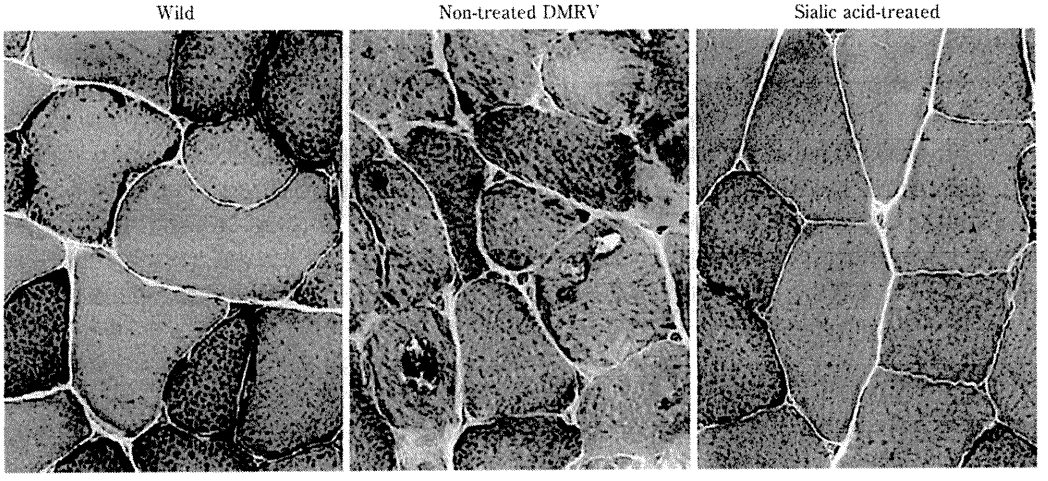

Fig. 2 Muscle pathology of DMRV model mice with or without sialic acid supplementation. Without sialic acid treatment, DMRV mice show numerous rimmed vacuoles, in addition to marked variation in fiber size, at age 55 weeks. These features are essentially identical to those seen in human DRMV/HIBM patients. In contrast, with sialic acid treatment, DMRV mice show virtually no abnormality, clearly demonstrating that sialic acid can preclude DRMV/HIBM. ManNAc and sialyllactose also showed essentially the same efficacy. Modified Gomori trichrome stain. Gastrocnemius muscles.

ティブ・スプライシングにより，LAMP-2A，2B，2Cの3つのアイソフォームが作られる．

一例の患者では，フレーム・シフト変異がエクソン9Bにあり，LAMP-2Bアイソフォームのみ影響がある．この例の骨格筋をもちいたウエスタン・ブロットでは，極微量のバンドが検出された[10]．このバンドはLAMP-2Aアイソフォームを反映していると考えられる．以上の実験結果は，骨格筋や心筋で，LAMP-2Bが主要なアイソフォームであるという事実と良く一致している．また，この患者は，明らかな精神遅滞はないものの，心筋症やミオパチーは他の患者と同程度と考えられることから，LAMP-2B欠損のみでもDanon病がおこりうることを示している．近年オートファジーには様々な様態があることが知られてきており，この中で，ある種の蛋白質はシャペロンとLAMP-2Aを介してライソゾーム内に直接取り込まれて分解されるとされている[13]．この，シャペロン介在性オートファジー（chaperone-mediated autophagy：CMA）と呼ばれる機構は，LAMP-2そのものを欠くDanon病においてはまったく機能していないはずであり，Danon病の病態の一端はCMAがおこらないことによるものだとの仮説も成立しえる．しかし，LAMP-2B欠損のみでDanon病を発症する患者の存在は，少なくとも骨格筋や心筋においては，CMAは主要な役割を果たしていない可能性を示唆している．

LAMP-2ノックアウトマウスの検討結果からは，LAMP-2欠損により，一部のライソゾーム酵素のミスターゲティングにより，ライソゾームへと正しく運ばれないことが知られている[14]．もしこのことがDanon病の主要な病態であるならば，Danon病も一部のライソゾーム酵素の部分欠損症との解釈も成り立つ．また，最近では，LAMP-2がオートファゴソームの成熟に関係しているとの報告もある[15]．しかし，Danon病の詳細な病態，とくに，なぜAVSFが形成されるのかは，まったく不明であり，更なる検討が必要である．

2．その他のAVSFミオパチー

a）過剰な自己貪食をともなうX連鎖性ミオパチー

過剰な自己貪食をともなうX連鎖性ミオパチー（X-linked myopathy with excessive autophagy：XEMA）は，当初フィンランドから報告された比較的軽症のミオパチーである[16]．Danon病とことなり，骨格筋のみが侵され，心筋や脳は侵されない．60歳を過ぎても歩行可能な例が多く，Danon病と比較して予後良好とされている．筋病理学的には，Danon病と同様にAVSFを呈する．加えて，電顕上，基底膜が重層化し，同部位にカルシウムと補体C5b-9の沈着がみとめられる[17][18]．最近，本疾患が，ライソゾーム腔内の酸性化に決定的な役割を有するvacuolar ATPaseのアセンブリ因子をコードする*VMA21*の変異によることが明らかとなった[19]．XMEA例では，実際にライソゾーム内の酸性度が低下していることが報告されている．Danon病もXMEAもともにライソゾーム機能異常により発症する疾患であることは興味深い．これとは対照的に，後で述べるRVMは，基本的にライソゾーム外に根本的原因が存在する．

b）乳児型/先天型自己貪食空胞性ミオパチー

われわれは，これまでに，乳児重症型AVM[20]やX連鎖性を示唆する家族歴を有し，生下時より先天性ミオパチー様の臨床症状を呈する兄弟例を報告している[21]．この例はAVSF

を有しており，Danon病やXMEA等が鑑別診断として挙がったが，発症年齢も重症度もことなることから，別のAVMと捉えられる．筋病理学的には，AVSFをみとめるとともに(Fig. 1)，基底膜の重層化と補体C5b-9の筋鞘膜への沈着があり，どちらかというとXMEAに近い病態が示唆される．

c）成人型自己貪食空胞性ミオパチー

NonakaIらは，成人で骨格筋内に多数のAVSFを呈し，脳，心，肝，肺，腎など多臓器が侵された例を報告しているが，その病因・病態はまったく不明である[22]．今後もさらに，AVSFを呈するミオパチーが新たにみいだされていくものと思われる．

3. 縁取り空胞をともなう遠位型ミオパチー

a）臨床症状

RVMの代表として，縁取り空胞をともなう遠位型ミオパチー（distal myopathy with rimmed vacuoles：DMRV）の研究を取り上げる．本疾患は，欧米では，遺伝性封入体ミオパチー（hereditary inclusion body myopathy：HIBM）と呼ばれている[23,24]．常染色体劣性の筋疾患であり，男女ほぼ平等に侵されて，通常15歳～40歳で発症する．前脛骨筋と大腿後面筋が侵されやすく，大腿四頭筋は病後期まで比較的良好に保たれる．前脛骨筋の障害を反映して，多くの患者で下垂足が初発症状である．平均的には発症後約12年程度で歩行不能となり，車椅子状態となるが，最近は，臨床的重症度や進行の速さにはかなりばらつきがあることが知られるようになってきている．

患者数は日本国内に150人から400人程度と予想され，超希少疾病である．

b）筋病理

縁取り空胞と管状線維性封入体の出現が特徴である．免疫染色をおこなえば，β-アミロイド沈着やタウ蛋白質リン酸化といった神経変性疾患に似た変化もみとめられる[20,21]．縁取り空胞は，電顕的には自己貪食空胞の集塊であり，DMRVは自己貪食空胞性ミオパチーとしての側面も有している[3]．これに加えて，小角化線維様の萎縮線維をみとめる．われわれが作製したDMRVモデルマウスでの解析結果からは，萎縮線維がまず先行して出現し，次にβ-アミロイドが沈着し，その後，縁取り空胞やリン酸化タウが出現してくることが明らかになっている[25,26]．

c）原因遺伝子

2001年にイスラエルのグループによりHIBMの原因遺伝子がシアル酸生合成経路律速酵素をコードする*GNE*であることが明らかにされた[27]．本邦DMRV患者でも同様に*GNE*変異がみいだされることから，DMRVとHIBMは同一疾患であることが確定した[28]．これまでに見つかった患者のアレルの95%以上がミスセンス変異であり，null変異を両アレルに有する例はみいだされていない．これは，*Gne*ノックアウトマウスは胎生致死である事実とよく合致している[29]．本邦ではp.V572L変異が一番多く，p.D176V変異が2番目に多い．

d）分子病態とモデルマウス

患者の血液，筋組織，線維芽細胞，筋管細胞で，シアル酸量が低下し，とくに筋管細胞においては，細胞表面のシアリル化が低下している[30]．さらに，培養線維芽細胞および筋管細胞において，GNE代謝産物の*N*-アセチルマンノサミン（ManNAc）または主要なシアル酸であるノイラミン酸（NeuAc）の投与により，これらが効率よく細胞内に取り込まれてシアリル化状態の回復がみとめられることを示した[30]．これは，仮にシアリル化減少がDRMVの本態であるならば，*in vitro*ではすでに治療可能であることを示している．

われわれは*Gne*ノックアウトのヘテロ接合体マウスとヒト*GNE*p.D176V変異体を発現するトランスジェニックマウスを作製して掛け合わせ，ヒト*GNE*p.D176Vを*GNE*ノックアウトバックグラウンドで発現する*Gne*$^{-/-}$h*GNE* D176V-Tgマウス（DMRVモデルマウス）を作製した[25]．われわれのマウスは，生後21週以降より，体重減少と筋萎縮を，31週より筋線維内のアミロイド沈着，41週よりリン酸化タウ，管状線維性封入体，縁取り空胞の出現をみとめ，更に，全身臓器でのシアル酸量低下と軽度の血清CK値上昇をみとめた[25,26]．これは，われわれのマウスが，ヒトDMRVを臨床的・病理学的・生化学的に再現する世界ではじめてのDMRV/HIBMモデルマウスであることを示している．加えて，われわれのマウスにより，アミロイド沈着が縁取り空胞よりも時間的に先に形成されることがはじめて明らかとなり，病態の一端が解明された[25]．

われわれのマウスでの解析により，DMRV/HIBMでみとめられる縁取り空胞形成はかなり下流の現象であることが明らかとなった．これは，相当幅広い疾患に縁取り空胞がみとめられる事実と良く合致している．この点は，AVSFを呈するミオパチーがライソゾーム機能異常を原因としていることと対照的であり，興味深い．

e）治療法開発

NeuAcやManNAcは静注すると約2分で尿中に排泄されてしまうことが良く知られている．そこで，正常マウスで腹腔内投与と経口投与を比較したところ，経口投与の方が尿中への排泄速度が遅く，さらに，投与2時間後の血中濃度も高かった．マウスは一日に約12回飲水をおこなうことから，自由飲水による経口投与をおこない，その治療効果を検討した[31]．

まず，まだ症状を呈していない時期の15週前後のDMRVマウスに対して，3つのことなる投与量（20, 200, 2,000mg/kg体重/日）でManNAcを与えたところ，いずれの用量においても，無治療であれば，ほぼすべての症状が出そろう55週の時点でも症状がみとめられなかった[31]．そこで，この最小量をもちい，ManNAcに加えて，NeuAc，シアル酸結合物であるシアリル乳糖の投与を同様のスケジュールでおこなった．その結果，どの薬剤においても，ManNAcと同様に，55週の時点でほぼ完全にDMRV発症を抑制できた．病理学的にも，筋線維萎縮，β-アミロイド沈着，縁取り空胞形成などの変化はいずれもみとめなかった(Fig. 2)．肝や腎などへの毒性もとくにみとめられなかった[31]．これらの結果は，GNE代謝産物が

DMRVに対して有効であることを明確に示すと同時に，確かに低シアル酸状態がDMRVの原因であることを明確に示した点でも意義が大きい．

これらの結果を踏まえると，当然，次はヒトでの検討，すなわち臨床試験ということになる．本邦でおこなわれる希少疾病薬開発の大半は，既存薬の適応拡大または欧米での既承認薬の国内承認を目的とするものである．われわれの知るかぎり，これまで，日本の研究室からの基礎研究成果に基づいて，DMRVのような「超」希少疾病に対する治療薬の開発が，原薬製造の段階から国内でおこなわれたことはない．DMRVの治療薬開発は，本邦における今後の希少疾病薬開発研究の試金石となると考えられる．

まとめ

AVMは，その疾患概念が徐々に受け入れられつつあり，今後はさらにあらたな疾患がみいだされていくことになると考えられる．AVSFを呈するミオパチーはDanon病とXMEAの原因遺伝子が明らかとなり，ともにライソゾーム機能異常を原因としている点で共通している．一方，DMRVなどのRVMはライソゾーム外に根本的原因があり，その下流現象として自己貪食が惹起されている可能性が高い．いずれにせよ，今後さらに病態が解明されて治療法開発が進むことになるであろうが，このような「超」希少疾病の治療薬開発に対して，本邦はどのようなスタンスで望んでいくのか，幅広い議論が必要であろう．

謝辞：AVM研究を始めるきっかけをお与え下さるとともに，日頃から暖かいご指導を賜っております国立精神・神経センター病院名誉院長の埜中征哉先生，Danon病研究でご指導を仰いだ米国コロンビア大学神経内科Michio Hirano先生ならびにSalvatore DiMauro先生，そして，いつも一緒に研究を進めてくれている国立精神・神経センター神経研究所疾病研究第一部の過去と現在の同僚，とくに昼夜を厭わず実験を積み重ねてDMRV治療開発につながる重要な成果を挙げたMay Malicdan医師と野口悟室長に感謝いたします．また，一連の研究にご協力下さった主治医の先生方，患者およびご家族の方々，遠位型ミオパチー患者会の方々に感謝いたします．

文　献

1) Nishino I. Autophagic vacuolar myopathy. Semin Pediatr Neurol 2006;13:90-95.
2) Nishino I. Autophagic vacuolar myopathy. Curr Neurol Neurosci Rep 2003;3:64-69.
3) Danon MJ, Oh SJ, DiMauro S, et al. Lysosomal glycogen storage disease with normal acid maltase. Neurology 1981;31:51-57.
4) Sugie K, Yamamoto A, Murayama K, et al. Clinicopathological features of genetically confirmed Danon disease. Neurology 2002;58:1773-1778.
5) Schorderet DF, Cottet S, Lobrinus JA, et al. Retinopathy in Danon disease. Arch Ophthalmol 2007;125:231-236.
6) Prall FR, Drack A, Taylor M, et al. Ophthalmic manifestations of Danon disease. Ophthalmology 2006;113:1010-1013.
7) Sugie K, Noguchi S, Kozuka Y, et al. Autophagic vacuoles with sarcolemmal features delineate Danon disease and related myopathies. J Neuropathol Exp Neurol 2005;64:513-522.
8) Murakami N, Goto Y-I, Itoh M, et al. Sarcolemmal indentation in cardiomyopathy with mental retardation and vacuolar myopathy. Neuromuscul Disord 1995;5:149-155.
9) Muntoni F, Catani G, Mateddu A, et al. Familial cardiomyopathy, mental retardation and myopathy associated with desmin-type intermediate filaments. Neuromuscul Disord 1994;4:233-241.
10) Nishino I, Fu J, Tanji K, et al. Primary LAMP-2 deficiency causes X-linked vacuolar cardiomyopathy and myopathy (Danon disease). Nature 2000;406:906-910.
11) Tanaka Y, Guhde G, Suter A, et al. Accumulation of autophagic vacuoles and cardiomyopathy in LAMP-2-deficient mice. Nature 2000;406:902-906.
12) Fukuda M. Biogenesis of the lysosomal membrane. Subcell Biochem 1994;22:199-230.
13) Kaushik S, Cuervo AM. Chaperone-mediated autophagy. Methods Mol Biol 2008;445:227-244.
14) Eskelinen EL, Illert AL, Tanaka Y, et al. Role of LAMP-2 in lysosome biogenesis and autophagy. Mol Biol Cell 2002;13:3355-3368.
15) Saftig P, Beertsen W, Eskelinen EL. LAMP-2: a control step for phagosome and autophagosome maturation. Autophagy 2008;4:510-512.
16) Kalimo H, Savontaus M-L, Lang H, et al. X-linked myopathy with excessive autophagy: a new hereditary muscle disease. Ann Neurol 1988;23:258-265.
17) Villanova M, Louboutin JP, Chateau D, et al. X-linked vacuolated myopathy: complement membrane attack complex on surface membranes of injured muscle fibers. Ann Neurol 1995;37:637-645.
18) Louboutin JP, Villanova M, Lucas-Heron B, et al. X-linked vacuolated myopathy: membrane attack complex deposition on muscle fiber membranes with calcium accumulation on sarcolemma. Ann Neurol 1997;41:117-120.
19) Ramachandran N, Munteanu I, Wang P, et al. VMA21 deficiency causes an autophagic myopathy by compromising V-ATPase activity and lysosomal acidification. Cell 2009;137:235-246.
20) Yamamoto A, Morisawa Y, Verloes A, et al. Infantile autophagic vacuolar myopathy is distinct from Danon disease. Neurology 2001;57:903-905.
21) Yan C, Tnaka M, Sugie K, et al. A new congenital form of

X-linked autophagic vacuolar myopathy. Neurology 2005; 65:1132-1134.
22) Kaneda D, Sugie K, Yamamoto A, et al. A novel form of autophagic vacuolar myopathy with late-onset and multiorgan involvement. Neurology 2003;61:128-131.
23) Nonaka I, Noguchi S, Nishino I. Distal myopathy with rimmed vacuoles and hereditary inclusion body myopathy. Curr Neurol Neurosci Rep 2005;5:61-65.
24) Malicdan MC, Noguchi S, Nishino I. Recent advances in distal myopathy with rimmed vacuoles (DMRV) or hIBM: treatment perspectives. Curr Opin Neurol 2008;21:596-600.
25) Malicdan MC, Noguchi S, Nonaka I, et al. A Gne knockout mouse expressing human GNE D176V mutation develops features similar to distal myopathy with rimmed vacuoles or hereditary inclusion body myopathy. Hum Mol Genet 2007;16:2669-2682.
26) Malicdan MC, Noguchi S, Hayashi YK, et al. Muscle weakness correlates with muscle atrophy and precedes the development of inclusion body or rimmed vacuoles in the mouse model of DMRV/hIBM. Physiol Genomics 2008;35:106-115.
27) Eisenberg I, Avidan N, Potikha T, et al. The UDP-N-acetylglucosamine 2-epimerase/N-acetylmannosamine kinase gene is mutated in recessive hereditary inclusion body myopathy. Nat Genet 2001;29:83-87.
28) Nishino I, Noguchi S, Murayama K, et al. Distal myopathy with rimmed vacuoles is allelic to hereditary inclusion body myopathy. Neurology 2002;59:1689-1693.
29) Schwarzkopf M, Knobeloch KP, Rohde E, et al. Sialylation is essential for early development in mice. Proc Natl Acad Sci USA 2002;99:5267-5270.
30) Noguchi S, Keira Y, Murayama K, et al. Reduction of UDP-N-acetylglucosamine 2-epimerase/N-acetylmannosamine kinase activity and sialylation in distal myopathy with rimmed vacuoles. J Biol Chem 2004;279:11402-11407.
31) Malicdan MC, Noguchi S, Hayashi YK, et al. Prophylactic treatment with sialic acid metabolites precludes the development of the myopathic phenotype in the DMRV-hIBM mouse model. Nat Med 2009;15:690-695.

Abstract

Eludication of pathomechanism of and development of therapy for autophagic vacuolar myopathies

Ichizo Nishino, M.D.
Department of Neuromuscular Research, National Institute of Neuroscience,
National Center of Neurology and Psychiatry (NCNP)

Autophagic vacuolar myopathy (AVM) is an entity defined by the presence of autophagic vacuoles on muscle pathology. There are two emerging categories in AVM in addition to the best characterized Pompe disease.

One is Danon disease and its related disorders, which are characterized by autophagic vacuoles with unique sarcolemmal features (AVSF). AVSF express virtually all sarcolemmal proteins, in addition to acetylcholinesterase, on their vacuolar membranes. Danon disease is caused by primary deficiency of a lysosomal membrane protein, LAMP-2. Interestingly, in this disease, the number of AVSF increases as the patients age. Other AVSF myopathies include X-linked myopathy with excessive autophagy which is now known to be caused by *VMA21* mutations.

The other AVM is typified by the presence of rimmed vacuoles, which are actually clusters of autophagic vacuoles on electron microscopy. One of the well known diseases in this group is distal myopathy with rimmed vacuoles (DMRV), also called hereditary inclusion body myopathy (HIBM). DMRV is caused by mutations in *GNE* gene that encode a rate-limiting enzyme in the sialic acid biosynthetic pathway. Interestingly, in DMRV model mice, sialic acid supplementation almost completely precluded the disease phenotype, indicating that decreased sialic acid is the cause of myopathic phenotype and sialic acid supplementation can prevent the disease process.

Interestingly, both genetically diagnosable AVSF myopathies are primarily due to lysosomal dysfunctions. In contrast, rimmed vacuoles are secondarily caused by extra-lysosomal defects, such as hyposialylation in DMRV/HIBM, and are formed at later stages of the disease.

(Clin Neurol 2010;50:1-6)

Key words: autophagy, distal myopathy, hereditary inclusion body myopathy, rimmed vacuole, sialic acid, GNE

of p62 positive aggregates correlate pretty well with myofiber atrophy. In general the degradation systems appear to be still functioning in these patients and seem to contribute positively to counteract disease progression. In conclusion, present data underline the role of unproductive autophagy and accumulation of aggregate-prone ubiquitinated proteins in the pathogenesis of GSDII, especially in more severely affected patients.

SM202. An exploratory analysis of scoliosis in 182 children and adults with Pompe disease from the Pompe Registry

Merlini, Luciano[1]; Case, Laura[2]; Kishnani, Priya[2]; Muller-Felber, Wolfgang[3]; Roberts, Mark[4]; van der Ploeg, Ans[5]; Prasad, Suyash[6]

[1]University of Ferrara, Ferrara, Italy; [2]Duke University Medical Center, Durham, United States; [3]Friedrich-Baur Institute, Munich, Germany; [4]Withington Hospital, Manchester, United Kingdom; [5]Erasmus Medical Center, Rotterdam, Netherlands; [6]Genzyme Corporation, Cambridge, United States

The prevalence of scoliosis and its relationship with respiratory function are explored in patients enrolled in the Pompe Registry. Scoliosis status was reported for 575 patients, 182 of whom had scoliosis (25 children age 0 to < 2 years or ≥ 2 to < 13 years; 24 teenagers age ≥ 13 to < 20 years, and 133 adults age ≥ 20 years).

Children age ≥ 2 years with scoliosis had a mean age at Pompe symptom onset of 1.1 years, identical to children without scoliosis. Teenagers with scoliosis had a mean age at symptom onset of 5.8 years compared with 9.1 years in teenagers without scoliosis. Adults with scoliosis had mean age at symptom onset of 25.3 years compared with 32.8 years in adults without scoliosis.

Among the subset of patients with FVC data, children age ≥ 2 years (n = 6) and teenagers (n = 9) with scoliosis had lower % predicted forced vital capacity (FVC) upright median scores (68.0% and 59.0%, respectively) than those in similar age groups without scoliosis (15 children, 5 teenagers; 77.0% and 91.1%, respectively). Children age ≥ 2 years with scoliosis (n = 3) had lower median % predicted FVC supine scores than those in similar age groups without scoliosis (n = 5) (47.0% versus 70.0%, respectively). Supine scores for teenagers without scoliosis were unavailable. Among adults, FVC % predicted upright and supine median scores were similar regardless of scoliosis status.

Further analysis and collection of detailed scoliosis and respiratory function data is needed to better understand this relationship and how scoliosis affects quality of life in patients with Pompe disease.

SM203. Quantitative metabolome profiling of biopsied muscle in the patients with glycogen storage diseases using capillary electrophoresis mass spectrometry

Fukuda, Tokiko[1]; Sugie, Yoko[2]; Sugie, Hideo[3]

[1]Jichi Medical University, Tochigi, Japan; [2]Hamamatsu Medical University, Pediatrics, Hamamatsu, Japan; [3]Jichi Medical University, Pediatrics, Shimotsuke, Japan

Metabolome analysis has lately been applied for the characterization of disease-specific metabolism. Recently developed capillary electrophoresis time-of-flight mass spectrometry (CE-TOFMS) has enabled quantitative analysis of charged metabolites by the simultaneous measurement of their levels in tissues. In order to characterize the metabolism of muscular glycogen storage diseases (M-GSD), and also to evaluate whether CE-TOFMS could be a valuable diagnostic tool for M-GSD, we applied CE-TOFMS to measure the metabolites involved in energy production in the muscles of M-GSD. Biopsied muscles were obtained from each patient with GSDIIa, IIb, III, V, VII, and phosphoglycerate kinase (PGK) deficiency. Histologically normal muscles from three myopathy patients with normal CK values were used as controls. We identified 10 metabolites involved in glycolysis, 8 in TCA cycle, and 4 in pentose phosphatase pathway. The amounts of glycolytic intermediates locating downstream of G-1-P in the glycolytic pathway were much less in muscles of GSD III and V than in control muscles, while the amounts of glycolytic intermediates locating upstream of FDP (G-6-P, G-1-P and F-6-P) and those locating upstream of 3-phosphoglycerate were significantly high in muscles of GSD VII and in PGK deficiency, respectively. There was no difference in the amounts of glycolytic intermediates between GSD II and controls. The amounts of the metabolites in TCA cycle were higher in muscles of GSD II than in controls. The metabolome analysis of biopsied muscles had clearly determined the blockage of the metabolic pathway. We conclude that this method could be a high through-put and good method for diagnosis in M-GSD.

SM204. Adult Pompe disease: bone mineral density before and after enzyme replacement therapy

Papadimas, George-Konstantinos[1]; Terzis, Gerasimos[2]; Methenitis, Spyridon[2]; Spengos, Konstantinos[2]; Papadopoulos, Constantinos[2]; Kavouras, Stavros[2]; Michelakakis, Helen[3]; Manta, Panagiota[2]

[1]University of Athens, Medical School, Neurology, Athens, Greece; [2]University of Athens, Athens, Greece; [3]'Ag. Sophia' Children's Hospital, Athens, Greece

Pompe disease is an autosomal recessive disorder caused by lysosomal α-glycosidase deficiency. The infantile form is characterized by cardiomegaly and severe muscle weakness with an early fatal outcome, while the adult form is usually milder with progressive muscle weakness and respiratory dysfunction. Bone mineral density (BMD) seems to be decreased in the infantile form leading to osteopenia and fractures, but data concerning the adult form of the disease are still limited. The aim of the present study is to evaluate BMD in patients with the adult form of Pompe disease before and after enzyme replacement therapy (ERT).

Body composition was examined by means of dual x-ray absorptiometry at baseline and after 9-12 months of ERT in five patients with the adult onset form of Pompe disease.

One patient had reduced BMD in total body, L2-L4 spine and femoral neck in the range of osteopenia, one other had reduced L2-L4 spine BMD and two patients had slightly reduced femoral neck BMD. After 9-12 months of ERT, BMD was not considerably altered in any patient.

A slight reduction of BMD among patients with the adult form of Pompe disease might be occasionally found. The short-

PEDIATRICS INTERNATIONAL Official Journal of the Japan Pediatric Society
Pediatrics International (2011) **53**, 129–130 doi: 10.1111/j.1442-200X.2010.03282.x

Letter to the Editor

Liver biopsy is an important procedure in the diagnosis of glycogen storage disease type IV

Tatsuki Mizuochi,[1] Akihiko Kimura,[1] Hiroshi Nishiura,[1] Yukihiro Inomata,[4] Hideaki Okajima,[4] Hideo Sugie,[6] Hiroshi Mitsubuchi,[5] Minoru Yagi[2] and Masayoshi Kage[3]

Departments of [1]Pediatrics and Child Health, and [2]Pediatric Surgery, and [3]Pathology, Kurume University School of Medicine, Kurume, and Departments of [4]Pediatric Surgery and Transplantation and [5]Pediatrics, Kumamoto University Graduate School of Medical Science, Kumamoto University, Kumamoto, and [6]Department of Pediatrics, Jichi Medical University and Jichi Children's Medical Center, Tochigi, Japan

Glycogen storage disease type IV (GSD IV) is a rare autosomal recessive metabolic disorder characterized by deficient glycogen branching enzyme (GBE) activity. This severe metabolic disease results in abnormal deposition of amylopectin-like glycogen in multiple organs, such as the liver, muscle, heart, and the nervous system.[1,2] This disease most frequently presents in the first few months of life, with hepatosplenomegaly and failure to thrive. This is followed by progressive liver cirrhosis with portal hypertension, ascites, esophageal varices, and death by 5 years of age.[3] Generally, diagnosis of GSD does not require liver biopsy. However it is difficult to diagnose GSD IV when symptoms extend to multiple organs. No specific treatment for this disease exists. Liver transplantation has been proposed as a treatment;[2,4,5] however, this may not improve extrahepatic manifestations in the same patients.[4]

We experienced a case of GSD IV in a 5-month-old boy who was born without complications after 38 weeks of gestation. He had no significant family history and developed normally until the age of 4 months, at which time he experienced high fever, tachypnea, and poor feeding. On admission to our hospital, he had hepatosplenomegaly with elevation of serum transaminases (aspartate aminotransferase [AST], 312 IU/l and alanine aminotransferase [ALT], 108 IU/l); hypotonia; cardiomegaly (cardiothoracic ratio, 67%); elevated white blood count (27 570/μl) and C-reactive protein (9.1 mg/dl). Ultrasonography revealed pericardial effusion and increased myocardial thickness. After admission, the patient rapidly developed signs of cardiomyopathy and respiratory distress accompanied by high fever and petechiae. However, serum creatine phosphokinase concentration was normal. Therefore, his cardiac findings may have been due to a respiratory problem, such as infection, or to a combination of abnormal deposition of amylopectin-like glycogen and infection. He was treated with respiratory therapy, antibiotics, γ-globulin, and a diuretic. However, his condition did not improve, and his liver function sharply deteriorated: AST, 729 IU/l; ALT, 146 IU/l; total bilirubin, 2.6 mg/dl; and prothrombin, 54% (normal range: >60%). At that time we were still unable to make a diagnosis so we carried out an open liver biopsy. We did not evaluate leukocytes.[5] The biopsy specimen showed periodic acid-Schiff-positive cytoplasmic inclusions, largely resistant to diastase digestion (Fig. 1). GBE activity in a sample from the specimen was very low (0.09 μmol Pi/min/mg protein; control, 1.2 ± 0.3), as measured in the laboratory of Dr H. Sugie.

From the above results, especially the histological findings from the biopsy, the patient was diagnosed as having GSD IV. He received a living-donor liver transplant from his mother at Kumamoto University Hospital. After transplantation, his symptoms, including abnormal liver function, cardiomyopathy, dyspnea, hypotonia, and petechiae, rapidly improved except for fever. Histological findings from the liver biopsy specimen, particularly the faintly stained basophilic inclusions in hepatocytes, were very useful and ultimately led to the diagnosis of GSD IV. We therefore consider liver biopsy very important for the diagnosis of this disease. However, it should be kept in mind that enzyme assay in the liver can be very tricky when the liver is cirrhotic.

We carried out living-donor liver transplant with the patient's mother as the donor. After liver transplantation, all disease manifestations except for fever abated. Resorption of extrahepatic deposits of abnormal glycogen has been demonstrated after liver transplantation;[6,7] the mechanism for resorption of deposits in organs apart from the liver remains unknown.

In conclusion, we report a 5-month-old boy with GSD IV, including fever of unknown origin both before and after liver transplantation, and emphasize the importance of liver biopsy in the diagnosis of GSD IV.

Correspondence: Akihiko Kimura, MD PhD. Department of Pediatrics and Child Health, Kurume University School of Medicine, 67 Asahi-machi, Kurume 830-0011, Japan. Email: hirof@med.kurume-u.ac.jp

Received 21 January 2010; revised 12 April 2010; accepted 8 September 2010.

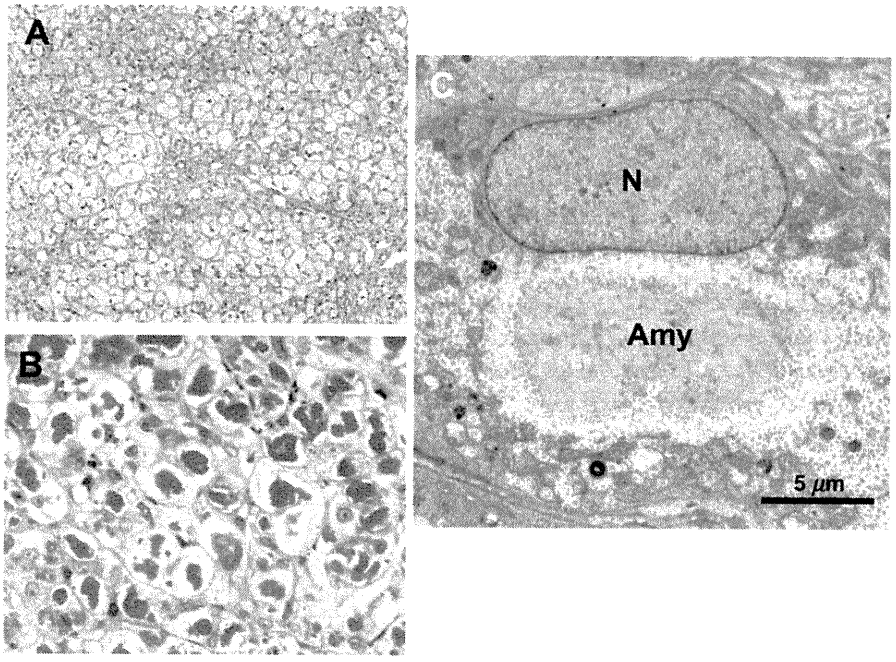

Fig. 1 Liver biopsy specimen from our patient with GSD IV. (a) Hepatocytes are enlarged and contain faintly stained basophilic cytoplasmic inclusions (hematoxylin–eosin stain, ×100). (b) The inclusions are periodic acid-Schiff-positive and diastase-resistant (×400). (c) Ultrastructurally, hepatocytes are occupied by large aggregates consistent with amylopectin (×10 000). N, nucleus; Amy, amylopectin.

References

1 Greene HL, Brown BI, McClenathan DT, Agostini RM Jr, Taylor SR. A new variant of type IV glycogenosis: deficiency of branching enzyme activity without apparent progressive liver disease. *Hepatology* 1988; **8**: 302–6.
2 Sokal EM, Von Hoof F, Alberti D *et al.* Progressive cardiac failure following orthotopic transplantation for type IV glycogenosis. *Eur. J. Pediatr.* 1992; **151**: 200–3.
3 Chen Y-T. Glycogen storage disease. In: Scriver CR, Beaudet AL, Sly WS, Valle D (eds). *The Metabolic & Molecular Bases of Inherited Disease*. McGraw-Hill, New York, 2001; 1521–51.
4 Rosenthal P, Podesta L, Grier R *et al.* Failure of liver transplantation to diminish cardiac deposits of amylopectin and leukocyte inclusions in type IV glycogen storage disease. *Liver Transpl. Surg.* 1995; **1**: 373–6.
5 Shin YS. Glycogen storage disease: clinical, biochemical, and molecular heterogeneity. *Semin. Pediatr. Neurol.* 2006; **13**: 115–20.
6 Starzl TE, Demetris AJ, Trucco M *et al.* Chimerism after liver transplantation for type IV glycogen storage disease and type I Gaucher's disease. *N. Engl. J. Med.* 1993; **328**: 745–9.
7 Davis MK, Weinstein DA. Liver transplantation in children with glycogen storage disease: controversies and evaluation of the risk/benefit of this procedure. *Pediatr. Transpl.* 2008; **12**: 137–45.

PEDIATRICS INTERNATIONAL Official Journal of the Japan Pediatric Society

Pediatrics International (2010) **52**, e150–e153 doi: 10.1111/j.1442-200X.2010.03073.x

Patient Report

Case of glycogen storage disease type VI (phosphorylase deficiency) complicated by focal nodular hyperplasia

Atsushi Ogawa,[1] Emi Ogawa,[1] Shigenori Yamamoto,[1] Tokiko Fukuda,[2] Hideo Sugie[2] and Yoichi Kohno[1]

[1]*Department of Pediatrics, Chiba University Graduate School of Medicine, Chiba-shi, Chiba and* [2]*Department of Pediatrics, Jichi Children's Medical Center Tochigi, Shimotsuke-shi, Tochigi, Japan*

Key words focal nodular hyperplasia, glycogen phosphorylase, glycogen storage disease.

Although it is well known that hepatic tumors often develop in patients with glycogen storage disease (GSD) types Ia and III, the formation of these tumors has not been reported in other forms of hepatic GSD. In this report, a patient with GSD type VI (phosphorylase deficiency; OMIM 232700) complicated with a hepatic benign tumor, focal nodular hyperplasia (FNH), is presented. This case indicates that regular check-ups for hepatic tumors are necessary, not only in patients with GSD types Ia or III, but also in patients with other forms of hepatic GSD.

Case Report

A female patient was referred to our hospital when she was 5 years of age for further investigation of hepatomegaly, which had been detected when she had visited a clinic when she was 5 years old. She was born to healthy non-consanguineous parents and had no history of hypoglycemia or nasal bleeding. On physical examination, her height was 101 cm (−1.5 SD) and her bodyweight was 16 kg (−1.0 SD). The liver was firm and palpable 7 cm below the right costal margin, whereas the spleen was not palpable. The results of a fasting blood test collected at that time were as follows: aspartate aminotransferase 37U/L, alanine aminotransferase 24U/L, blood glucose 85 mg/dL, lactate 6.2 mg/dL, uric acid 5.9 mg/dL, total cholesterol 229 mg/dL and triglyceride 88 mg/dL. A plain abdominal computed tomography (CT) scan showed an enlarged liver with a density considerably higher than that of the spleen (CT values: liver, 80; spleen, 42) (Fig. 1). Glucose and galactose loading tests were performed. The serum lactate level was not elevated when glucose was loaded, although it increased to a maximum of 56 mg/dL one hour after loading (normal <35 mg/dL). A glucagon loading test was performed after a 15-h fast, with the serum glucose level increasing from 71 to 128 mg/dL one hour after loading. On the basis of these data, GSD was suspected and accordingly the enzyme activities of hepatic GSD, that is, debranching enzyme, phosphorylase and phosphorylase b kinase, were measured in peripheral blood. The results of all these tests were normal (Table 1). Informed consent for a liver needle biopsy for measurement of enzyme activity was not obtained. Although the enzyme activity of phosphorylase b kinase measured in peripheral blood was normal, a tentative diagnosis of GSD type IX (phosphorylase b kinase deficiency) was made based on the physical, laboratory and radiological findings and the results of the loading tests. Regular check-ups including abdominal CT scans for potential formation of hepatic tumor were performed every year. The patient's growth curve showed that she attained mean values around the time of puberty. The results of blood tests obtained between 5 and 14 years of age were as follows (mean ± SD): uric acid 5.9 ± 0.6 mg/dL, total cholesterol 208 ± 21.0 mg/dL and triglyceride 198 ± 111 mg/dL.

When the patient was 15 years of age, the early phase of a contrast-enhanced abdominal CT scan revealed an enhanced lesion in the liver (Fig. 1). After obtaining informed consent, specimens were obtained by needle biopsy from the tumor and non-tumor part of the liver. Histological findings of the non-tumor specimen showed strong periodic acid-Schiff (PAS) staining in hepatocytes that disappeared following diastase treatment, findings compatible with GSD. Histology of the tumor specimen demonstrated pericellular fibrosis, compatible with the diagnosis of FNH (Fig. 2). Fibrous bands containing bile ductules were not observed in the specimens. Enzyme activities of hepatic GSD were measured using liver tissue from the non-tumor section, which revealed that phosphorylase enzyme activity was 2.3 nmol/min/mg protein, a value corresponding to 24% of normal. The enzyme activity of both debranching enzyme and phosphorylase b kinase was normal (Table 1). Informed consent for gene analysis of phosphorylase (*PGYL*) could not be obtained. We concluded that the patient's diagnosis was GSD VI (phosphorylase deficiency) complicated by FNH. We elected to forego surgical treatment in favor of long-term observation. The size of the tumor has been monitored regularly with ultrasonography. As of now, the tumor does not appear to be enlarging.

Discussion

In this report we present a patient with GSD type VI complicated by FNH. This is the first report of a hepatic tumor complication

Correspondence: Atsushi Ogawa, MD PhD, Department of Pediatrics, Chiba University Graduate School of Medicine, 1-8-1 Inohana, Chuo-ku, Chiba 260-8670, Japan. Email: aogawa@faculty.chiba-u.jp

Received 28 February 2009; revised 7 June 2009; accepted 9 July 2009.

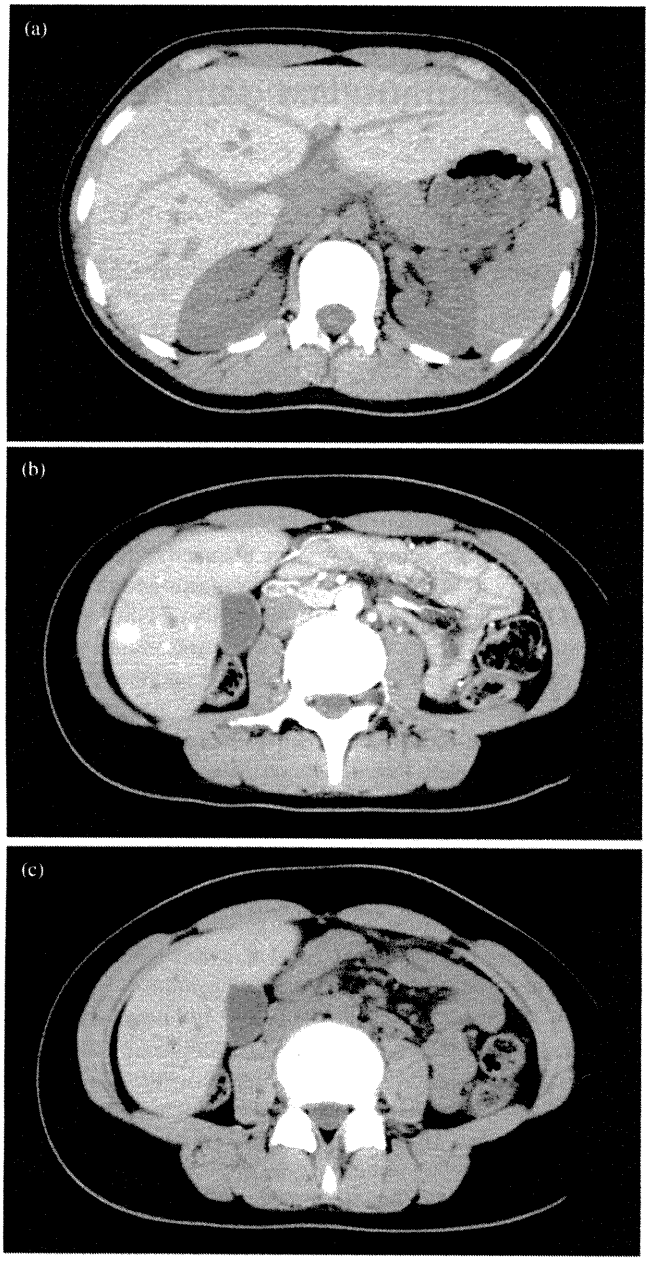

Fig. 1 (a) The findings of a plain abdominal computed tomography (CT) scan at 5 years of age. The CT value of the liver was markedly elevated compared with that of the spleen and kidneys. (b) The findings of the early phase of a contrast-enhanced abdominal CT scan at 15 years of age showing an enhanced lesion. (c) The findings of the same section as (b), without contrast enhancement.

in a patient with GSD type VI, a different hepatic form of GSD than types Ia or III. As hepatic tumors are often found in patients with GSD types Ia and III, regular check-ups for these tumors are performed routinely in these patients. However, this report indicates that regular check-ups for hepatic tumor are also necessary in patients with hepatic forms of GSD other than types Ia or III.

In patients with GSD type Ia, hepatic adenoma is the most common tumor described; however other tumors, including hepatocellular carcinoma (HCC),[1] described in patients with GSD III,[2] hepatoblastomas,[3] and FNH[4] have also been reported.

Hepatic adenomas are a benign tumor, consisting of a nodular proliferation of hepatocytes arranged in cords having no relationship to portal tracts. They often have a pushing border abutting against the surrounding liver. The hepatic adenoma has, on rare occasions, been known to progress to HCC,[1] and this is one of the most important reasons why regular check-ups and follow up after the discovery of an adenoma are necessary in a patient with GSD Ia. FNH is typically a single mass in an otherwise healthy liver characterized by central scarring that radiates between multiple nodules of regenerating parenchyma. Like the hepatic adenoma, it is also a benign tumor parenchyma but the potential for malignant transformation of FNH into HCC has not been demonstrated. However, a case of HCC arising within FNH has been reported recently[5] and this report emphasizes the importance of detecting FNH, even though the FNH itself is benign.

The mechanism of tumor formation in GSD type Ia is considered to occur by the following sequence.[6] Increased amounts of free fatty acids are released from adipose tissue, taken up by the liver and channeled into triglyceride formation. Malonyl-CoA is a key lipogenic intermediate in this process, which, in turn, causes inhibition of carnitine palmitoyltransferase I and limitation of mitochondrial beta-oxidation. This results in fatty acids being more likely to be channeled into extramitochondrial pathways, such as within peroxisomes, leading to an increase in hydrogen peroxide generation. This results in increased generation of free radicals that are capable of inflicting direct DNA damage, which may initiate the development of hepatic tumors. Although the patient reported here was diagnosed with GSD type VI, hypertriglyceridemia was almost always observed during the clinical course of the disease, similar to that seen in cases with type I GSD. We anticipate this would have resulted in increased generation of free radicals by the mechanism described above and could possibly have caused the formation of FNH we observed in the patient.

In our patient we observed a difference in phosphorylase activity between peripheral blood and liver tissue. Three isoforms of phosphorylase exist, that is, liver, brain and muscle. As the liver isoform is expressed in peripheral blood,[7,8] phosphorylase activity in peripheral blood and the liver should be the same. The reason why phosphorylase activity in peripheral blood and liver was different in our patient is not clear, although similar findings have been reported elsewhere.[9] Mutation analysis of the liver glycogen phosphorylase gene (*PYGL*) is necessary for further confirmation of this diagnosis.

In summary, we report a patient with GSD VI complicated with FNH. This case indicates that regular check-ups for hepatic tumors are necessary, not only in patients with GSD types Ia or III, but also in patients with other forms of hepatic GSD.

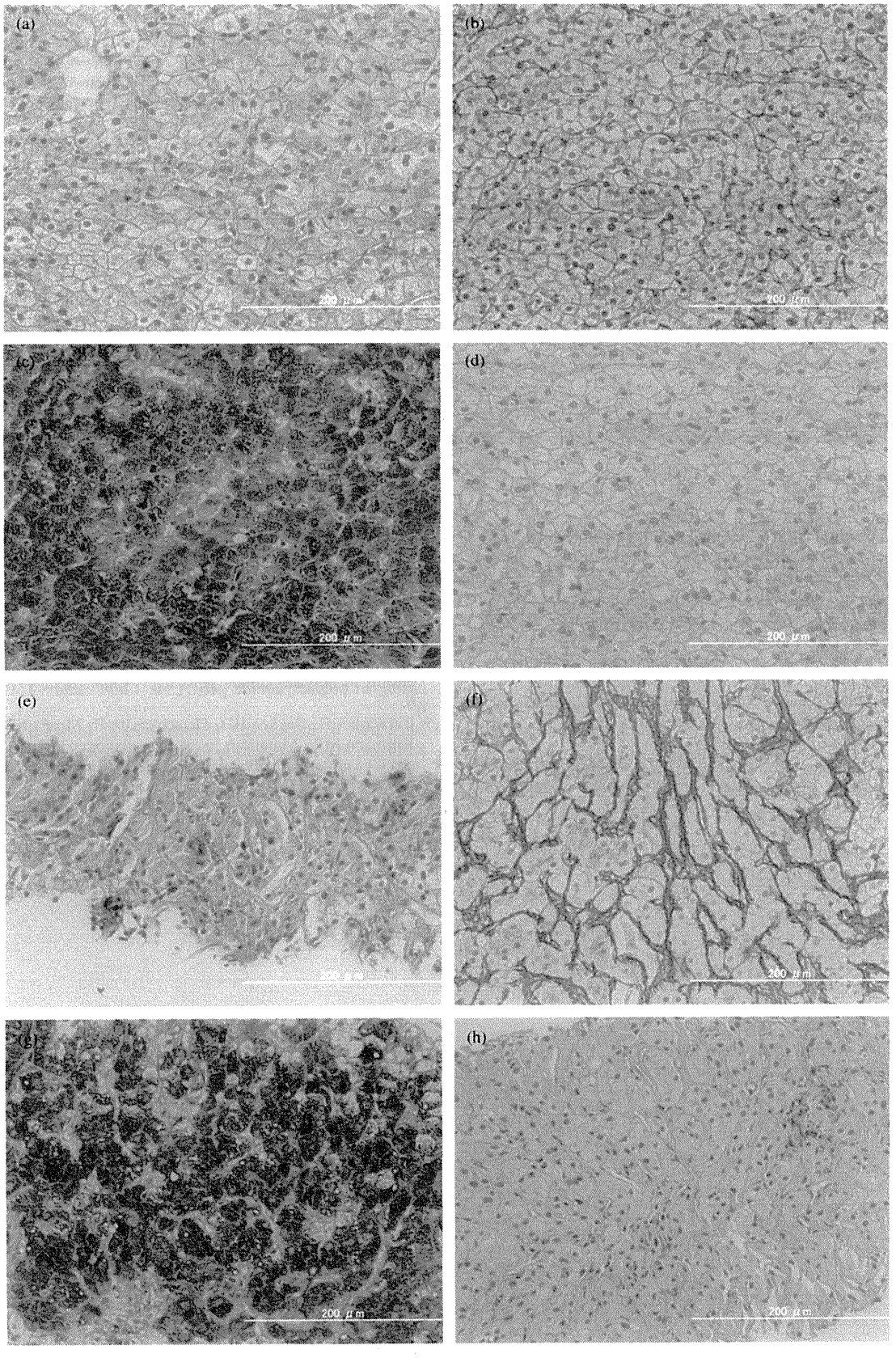

Fig. 2 Histological findings of the liver from (a–d) non-tumor and (e–h) tumor specimens. (a and e) Hematoxylin–eosin (HE) stain, (b and f) silver staining, (c and g) periodic acid-Schiff (PAS) staining and (d and h) PAS staining after diastase treatment. In the non-tumor specimen, the hepatocytes had (a) clear cytoplasm with (b) no fibrosis observed. (c and d) All the hepatocytes were stained strongly by PAS, which disappeared following diastase treatment. (e and f) In tumor specimens, pericellular fibrosis was observed, whereas fibrous bands in which bile ductules were proliferating were not. On the basis of the finding of pericellular fibrosis, a diagnosis of focal nodular hyperplasia was made. The original magnification was ×20.

Table 1 Results of enzyme activity measurements in the patient and controls

Peripheral blood	Patient	Control 1	Control 2	
Debranching enzyme	14.8	24.9	19.1	Nmole glucose/hour/mg
Phosphorylase	6.3	6.1	7.2	Nmole/min/mg
Phosphorylase b kinase	45.8	44.5	42.0	Nmole/min/g Hb
Liver	Patient	Controls		
Debranching enzyme	243.4	197.4 ± 32.8 (n = 10)		Nmole glucose/hour/mg
Phosphorylase	2.3	9.6 ± 1.7 (n = 10)		Nmole/min/mg
Phosphorylase b kinase	49.6	62.7 ± 11.8 (n = 9)		Nmole/min/mg

References

1 Franco LM, Krishnamurthy V, Bali D *et al.* Hepatocellular carcinoma in glycogen storage disease type Ia: A case series. *J. Inherit. Metab. Dis.* 2005; **28**: 153–62.
2 Demo E, Frush D, Gottfried M *et al.* Glycogen storage disease type III-hepatocellular carcinoma a long-term complication? *J. Hepatol.* 2007; **46**: 492–8.
3 Ito E, Sato Y, Kawauchi K *et al.* Type Ia glycogen storage disease with hepatoblastoma in siblings. *Cancer* 1987; **59**: 1776–80.
4 Takamura M, Mugishima H, Oowada M, Harada K, Uchida T. Type La glycogen storage disease with focal nodular hyperplasia in siblings. *Acta Paediatr. Jpn.* 1995; **37**: 510–3.
5 Petsas T, Tsamandas A, Tsota I *et al.* A case of hepatocellular carcinoma arising within large focal nodular hyperplasia with review of the literature. *World J. Gastroenterol.* 2006; **12**: 6567–71.
6 Lee PJ. Glycogen storage disease type I: Pathophysiology of liver adenomas. *Eur. J. Pediatr.* 2002; **161**(Suppl 1): S46–9.
7 Proux D, Dreyfus JC. Phosphorylase isoenzymes in tissues: Prevalence of the liver type in man. *Clin. Chim. Acta* 1973; **48**: 167–72.
8 Proux D, Vibert M, Meienhofer MC, Dreyfus JC. The isozymes of glycogen phosphorylase in human and rabbit tissues. II. Electrofocusing in polyacrylamide gels. *Clin. Chim. Acta* 1974; **57**: 211–6.
9 Burwinkel B, Bakker HD, Herschkovitz E, Moses SW, Shin YS, Kilimann MW. Mutations in the liver glycogen phosphorylase gene (PYGL) underlying glycogenosis type VI. *Am. J. Hum. Genet.* 1998; **62**: 785–91.

ELSEVIER

Brain & Development xxx (2009) xxx–xxx

BRAIN & DEVELOPMENT
Official Journal of the Japanese Society of Child Neurology

www.elsevier.com/locate/braindev

Original article

Study of *HOXD* genes in autism particularly regarding the ratio of second to fourth digit length

Yoko Sugie [a,*], Hideo Sugie [b], Tokiko Fukuda [b], Junko Osawa [a]

[a] *Department of Pediatrics, Hamamatsu University School of Medicine, Hamamatsu, Shizuoka, Japan*
[b] *Department of Pediatrics, Jichi Medical University and Jichi Children's Medical Center, Tochigi, Japan*

Received 30 December 2008; received in revised form 14 May 2009; accepted 16 May 2009

Abstract

Multiple genes are involved in the pathogenesis of autism. To study the causative gene, the relationship between autism endophenotypes and their closely related genes has been analyzed. There is a subgroup of autism spectrum disorder (ASD) in which the ratio of second digit length to fourth digit length (2D/4D) is low (short digit group, SDG). We studied the relationship between ASD and *HOXD* genes, which are located in the candidate locus for ASD and are associated with digit morphogenesis, with a particular focus on SDG. We analyzed 25 SNPs of *HOXD11*, *HOXD12*, and *HOXD13* in the subject of 98 ASD, 89 healthy controls, and 16 non-autistic patients (non-ASD). There was no significant difference in the genotype frequencies between the ASD and the healthy controls. However, the G-112T heterozygote in the promoter region of *HOXD11* was observed in only four patients with ASD and in none of the healthy controls or non-ASD subjects. Moreover, this *HOXD11* G-112T was observed in three of 11 SDG with ASD but in none of the 15 non-SDG patients with ASD. There were eight SDG patients among the non-ASD ones, but this polymorphism was observed in none of them. Considering the above results, it is expected that candidate genes will be further identified, using *HOXD11* G-112T polymorphism as a marker, by analyzing genes located near 2q in a larger number of ASD subjects with clinical signs of SDG.

Keywords: Autism; *HOXD*; 2D/4D; Endophenotype; Genetic polymorphism

This research was partly supported by a Grant-in-Aid for the Mentally and Physically Handicapped from the Ministry of Health, Labor and Welfare and the research Grant (14B-4-17) for Nervous and Mental Disorders from the Ministry of Health, Labor and Welfare, Japan. The authors declare that they have no competing interests.

1. Introduction

Autism is basically characterized by severely impaired social interaction and communication, and a limited range of activities and interests. As the diagnosis of autism is made on the basis of patients' behavioral characteristics, the disorder is not caused by only one factor. It is considered that various genetic and environmental factors are involved in the occurrence of autism, and their interactions are complex. In 1998, the International Molecular Genetic Study of Autism Consortium (IMGSC) reported their genome-wide linkage analysis of families in which there was more than one member with idiopathic autism [1]. On the basis of the results of a subsequent large-scale genome-wide scan, candidate

* Corresponding author. Address: Department of Pediatrics, Hamamatsu University School of Medicine, 1-20-1, Handayama, Higashi-ku, Hamamatsu 431-3192, Japan. Tel.: +81 53 435 2312; fax: +81 53 435 4311.
E-mail addresses: y-sugie@umin.ac.jp (Y. Sugie), sugie@jichi.ac.jp (H. Sugie), toki-fukuda@jichi.ac.jp (T. Fukuda), yusosawa@nifty.com (J. Osawa).

0387-7604/$ - see front matter © 2009 Elsevier B.V. All rights reserved.
doi:10.1016/j.braindev.2009.05.005

Please cite this article in press as: Sugie Y et al. Study of *HOXD* genes in autism particularly regarding the ratio of second to fourth digit length. Brain Dev (2009), doi:10.1016/j.braindev.2009.05.005

gene loci, including 7q21.2–q36.2, 16p12.1–p13.3, 6q14.3–q23.2, 2q24.1–q33.1, 17q11.1–q21.2, 1q21–q44, and 3q21.3–q29, were identified [2]. In an attempt to increase the linkage, a nearly homogeneous group was selected among patients with autism of heterogeneous causes. Autism patients were classified into subgroups or subsets in accordance with the phenotype of autism [3], such as through a quantitative trait locus (QTL) analysis of the constituent elements of endophenotypes in autism [4], and an ordered-subset analysis [5] was carried out. The ratio of second digit (2D) length to fourth digit (4D) length (2D/4D) is very low in some autism patients [6,7]. The *homeo box D (HOXD)* gene family is involved in skeletal morphogenesis, and correlations between digit length and the expression levels of *HOXD11*, *HOXD12*, and *HOXD13* have been observed [8,9]. In addition, *HOXD* genes form a cluster at 2q24.1–q33.1, which has been found to be a candidate locus by a genome-wide scan [3]. Therefore, we considered that digit length is one of the small physical signs of autism. Hence, we investigated the relationships between autism and polymorphism of *HOXD11*, *HOXD12*, and *HOXD13*. Moreover, we classified autism patients into two categories: patients with a low 2D/4D formed the short digit group (SDG), while the remaining patients formed the non-short-digit group (non-SDG). We also examined the genetic polymorphism of these three genes between SDG and non-SDG with autism and also between SDG with and without autism. No analysis of autism focusing on these relationships has been reported to date.

2. Subjects and methods

Seven patients with autism in the SDG were screened for the presence or absence of gene mutations in the exon and intron of *HOXD11*, *HOXD12*, and *HOXD13*, and for gene polymorphisms. The genotypic frequencies of the detected polymorphisms and the polymorphisms already listed in the GenBank were compared between the autism patients and the controls. Finally, the genotypes of the above polymorphisms of the autism patients in SDG were investigated.

2.1. Subjects

The subjects examined by genetic analysis in this study were 98 patients who visited the Department of Pediatrics, Hamamatsu University School of Medicine and Hamamatsu City Medical Center for Developmental Medicine, and who were diagnosed as having autism, PDD-NOS, and Asperger syndrome on the basis of the criteria in the Diagnostic and Statistical Manual of Mental Disorders (DSM-IV [10]). Patients with clear underlying diseases such as chromosomal abnormalities, tuberous sclerosis, and Fragile X syndrome were excluded from the study. The patients were of 82 males and 16 females with ages ranging from 5 years and 2 months to 31 years and 10 months (mean age: 12 years and 7 months). In terms of ethnicity, 95 patients had Japanese parents, 2 had Japanese fathers and Filipino mothers, and 1 had Bangladeshi parents. Eighty-nine subjects without any neurological abnormality served as healthy controls for gene analysis; all of them were Japanese and their sex and age were not determined. Thirty patients were also examined as disease controls, including 16 non-autistic patients, 14 mentally retarded patients, and 2 AD/HD patients, all of whom were Japanese.

2.2. Measurement of second and fourth digit lengths

A digital camera providing three-megapixel images was used for the measurement of the 2D and 4D lengths. Each subject's right hand was placed palm-up on a flat desk, and was photographed with the camera 20 cm above the hand. Three pediatric neurologists separately measured the 2D and 4D lengths from the line of the base to the tip of the digits three times using the image analyzing software Scion Image (NIH). The mean ratio of 2D length to 4D length (2D/4D) was calculated. In this study, patients with lower than the mean 2D/4D of the autism patients reported by Osawa et al., that is, a 2D/4D of 0.94 or lower, were classified as SDG [7].

2.3. Gene analysis

Seven patients with autism (6 males and 1 female) in the SDG were screened for the presence or absence of gene mutations and gene polymorphisms by the direct sequencing method. *HOXD11*, *HOXD12*, and *HOXD13* – each consisting of two exons and one intron – were searched for in a region from approximately 500 bp upstream, including a promoter, to approximately 500 bp downstream of the gene. Genomic DNA extracted from lymphocytes using a DNA extraction kit (Takara Co., Shiga, Japan) was used. DNA was amplified by PCR using a Taq PCR Core kit (QIAGEN Co., CA, USA), and the base sequence was obtained by the direct sequencing method. Genotypes were determined for single nucleotide polymorphism (SNP) in five loci that were newly found by this method in this study and for SNP in 20 loci that are listed in the online database GenBank (NCBL dbSNP). Genotypes in some loci were also determined by real-time PCR analysis using a TaqMan allelic discrimination assay (Applied Biosystems).

2.4. Statistical analysis

Genotypic frequency and allelic frequency of the autism patients were compared to those of the healthy con-

Please cite this article in press as: Sugie Y et al. Study of *HOXD* genes in autism particularly regarding the ratio of second to fourth digit length. Brain Dev (2009), doi:10.1016/j.braindev.2009.05.005

trol group using a χ^2 test or Fisher's exact test with SPSS 12.0J for a Windows-based System. A statistical significance level of $p \leqq 0.05$ was set.

3. Results

2D/4D was determined in 28 patients (24 males and 4 females) out of the 98 autism patients. Eleven patients (9 males and 2 females) of these 28 patients were classified as SDG. The clinical features of these patients, including sex, age, and the severity of mental retardation, are shown in Table 1. A high percentage of patients with severe mental retardation were observed in SDG with autism, whereas no patients with severe mental retardation were observed in non-SDG with autism. We also measured 2D/4D in 16 non-autistic patients in the disease control group, and 8 patients were classified as SDG and 8 patients as non-SDG. The results of the 2D/4D values of the 28 ASD and 30 non-ASD patients are shown in Fig. 1.

The results of the polymorphism analysis are shown in Table 2. No significant difference in polymorphism was observed between the autism patients and the healthy control group. However, with regarding to SNP in the promoter region of *HOXD11* G-112T, heterozygosity was observed in 4 autism patients, but not in the healthy or disease control group. The SNP in the promoter region of *HOXD12* -C226A and the SNP in

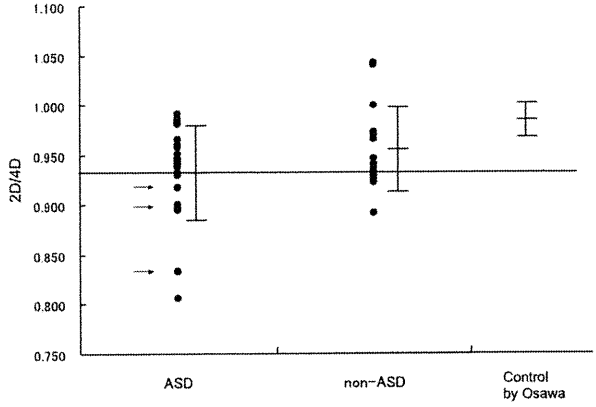

Fig. 1. 2D/4D values for the ASD28 cases and the non-ASD30 cases. Mean ± SD was presented. The M-ASD line is the average for the ASD cases; at or below this line is the SDG. As a reference, we showed the mean ± SD for normally healthy children as calculated by Osawa et al. [7]. The arrow indicates cases with *HOXD11* heterogeneity.

Table 1
Clinical features of patients.

	All the autistic disorder patients	Patients with 2D/4D determined		
		Total	SDG	NSDG
Number of patients	98	28	11	17
Sex				
Males:females	82:16 (5.1:1)	24:4 (5.5:1)	9:2 (4.5:1)	15:2 (7.5:1)
Age	5 y 2 m–31 y 10 m	5 y 4 m–31 y 10 m	8 y 1 m–31 y 10 m	5 y 4 m–16 y 7 m
Median	11 y 6 m	12 y 0 m	14 y 4 m	9 y 2 m
Mean	12 y 7 m	12 y 11 m	16 y 6 m	10 y 4 m
Family history: (3 generations)				
With[a]	22 (22.4%)	10 (35.7%)	3 (30.0%)	7 (41.2%)
Those with autism	7 (7.3%)	5 (17.9%)	2 (20.0%)	3 (17.4%)
Without	69 (70.4%)	16 (57.1%)	7 (70.0%)	7 (41.2%)
Mental retardation				
Without	10 (10.3%)	7 (25.0%)	2 (18.2%)	5 (29.4%)
Minor	21 (21.6%)	6 (21.4%)	2 (18.2%)	4 (23.5%)
Moderate	44 (45.4%)	10 (35.7%)	2 (18.2%)	8 (47.1%)
Severe	22 (22.7%)	5 (17.9%)	5 (45.5%)	0
Age at walk alone	9–48 m (91 cases)	9–48 m (26)	11–48 m (10)	9–18 m (16)
Median	13 m	12 m	12 m	12 m
Mean	13.9 m	14.3 m	18 m	12.9 m
Age at first word	10 m–6 y 10 m (80 cases)	11 m–6 y 10 m (25)	11 m–6 y 10 m (10)	1 y 3 m–3 y 5 m (15)
Median	1 y 6 m	1 y 6 m	1 y 6 m, 1 y 11 m	1 y 10 m
Mean	1 y 9 m	2 y 1 m	2 y 4 m	1 y 11 m
No. of patients 2 y or over	28	10	4	6
Age at first phrase	1 y 6 m–5 y 0 m (31 cases)	1 y 7 m–5 y 0 m (13)	2 y 6 m–5 y 0 m (5)	1 y 7 m–4 y 0 m (8)
Median	2 y 11 m	2 y 11 m	3 y 0 m	2 y
Mean	2 y 10 m	2 y 9 m	3 y 2 m	2 y 5 m
No. of patients 3 y or over	16	5	3	2

[a] Family history with psychiatric disorders including major depression, autism etc.

Please cite this article in press as: Sugie Y et al. Study of *HOXD* genes in autism particularly regarding the ratio of second to fourth digit length. Brain Dev (2009), doi:10.1016/j.braindev.2009.05.005

Table 2
Results of analysis of gene polymorphisms.

Gene	Location in gene	dtSNP ID	Allele	Frequency		Genotype	Frequency	
				Autism	Control		Autism	Control
HOXD11	Promoter		G	0.979	1	GG	0.959	1
			T	0.021	0	GT	0.042	0
						TT	0	0
	Intron	rs84746	A	0.711	0.721	AA	0.571	0.561
			C	0.289	0.288	AC	0.230	0.371
						CC	0.133	0.067
	Exon 2	rs863678	G	0.541	0.567	GG	0.316	0.292
			T	0.459	0.443	GT	0.449	0.551
						TT	0.235	0.157
	Exon2	rs6745764	A	0.214	0.18	AA	0.031	0.011
			G	0.786	0.82	AG	0.367	0.337
						GG	0.602	0.652
HOXD12	Promoter		A	0.041	0.028	AA	0	0
			C	0.959	0.972	AC	0.082	0.056
						CC	0.918	0.944
	Promoter		G	0.929	0.955	GG	0.929	0.955
			T	0.071	0.045	GT	0.071	0.045
						TT	0	0
	Exon 1	rs847151	A	0.041	0.028	AA	0	0
			G	0.959	0.972	AG	0.082	0.056
						GG	0.918	0.944
HOXD13	Promoter	rs847196	C	0.893	0.938	CC	0.786	0.876
			G	0.107	0.061	CG	0.214	0.124
						GG	0	0
	Promoter		A	0.082	0.107	AA	0	0
			T	0.918	0.893	AT	0.163	0.213
						TT	0.837	0.787
	Exon 1		C	0.985	0.989	CC	0.969	0.978
			T	0.015	0.011	CT	0.031	0.022
						TT	0	0
	Exon 1	rs2518053	A	0.408	0.455	AA	0.173	0.235
			G	0.592	0.545	AG	0.469	0.438
						GG	0.357	0.326
	Intron	rs847194	A	0.684	0.657	AA	0.459	0.404
			C	0.316	0.343	AC	0.449	0.506
						CC	0.092	0.09

SNP with no polymorphism detected in the present cases analyzed among the SNPs listed at the GenBank

HOXD11	Promoter	rs2736846	*HOXD13*	Exon 1	rs847195
	Intron	rs2736847		Exon 1	rs13392701
	Exon 2	rs12995279		Intron	rs847193
	Exon2	rs12995280		Intron	rs847192
HOXD12	Exon 1	rs2551807		Exon 2	rs28928892
	Exon2	rs2553776		Exon 2	rs28933082
				Exon 2	rs28928891

exon 1 of *HOXD12* (rs847151, G364A) showed a nearly complete linkage disequilibrium. Heterozygosity for both *HOXD12* -C226A and *HOXD12* G364A was observed in five healthy controls and eight autism patients. Furthermore, all of the five controls heterozygous for *HOXD12* -C226A and *HOXD12* G364A were homozygous for *HOXD11* -G112G. On the other hand, of the eight autism patients heterozygous for both *HOXD12* -C226A and *HOXD12* G364A, four were homozygous and four were heterozygous for *HOXD11* G-112T. Taken together, heterozygosity in all the three loci *HOXD11* G-112T, *HOXD12* -C226A, and *HOXD12* G364A was found in four autism patients but not in the healthy controls. Table 3 shows the relationships between the polymorphisms in these three loci for two cases: SDG and non-SDG with autism and SDG and non-SDG without autism. Of the four patients heterozygous for *HOXD11* G-112T, three in whom digit length was measured were classified into SDG with autism and the rest was unknown. The clinical type of ASD of the patients with having *HOXD11* heterogeneity was classified as autistic disorder in all cases. No patients

Please cite this article in press as: Sugie Y et al. Study of *HOXD* genes in autism particularly regarding the ratio of second to fourth digit length. Brain Dev (2009), doi:10.1016/j.braindev.2009.05.005

Table 3
Frequency of *HOXD* gene polymorphisms between SDG and NSDG patients with or without autism.

Gene	dbSNP ID	Genotype	Autistic patients			Normal	Non-autistic	
			Total	SDG	NSDG	Control	SDG	NSDG
HOXD11		GG	94	8	17	89	8	8
		GT	4	3	0	0	0	0
HOXD12		CC	90	8	17	84	8	8
		AC	8	3	0	5	0	0
HOXD12	rs847151	GG	90	8	17	84	8	8
		AG	8	3	0	5	0	0

heterozygous for *HOXD11* G-112T were observed among the 16 non-autistic disease controls including the eight patients with SDG.

4. Discussion

In genetic research for autism, some studies have been conducted that focused mainly on language development skills (e.g., age at first word, age at first phrase, onset of first phrase >36 months, and nonverbal communication) skill. Other studies have focused on the establishment of motor language development, bladder and bowel control milestones, developmental regression, repetitive/stereotyped behavior, restricted behavior, interest, and activity [2–4,11–13].

Manning et al. [6] reported that 2D/4D is low in autism and Asperger syndrome. In Japan, Osawa et al. [7] reported a higher incidence of low 2D/4D in autism patients than in healthy children. From their report, we assumed that it is possible to consider a low 2D/4D as a specific feature in some autism patients. Such patients formed part of a group of subjects (SDG) for investigation in our study. It was assumed that SDG in autism may express one of the common features; hence, 2D/4D may be associated with one of the etiological genes of autism. Manning et al. [14] reported the findings of their 2D/4D measurement as follows: (1) there is a gender difference in 2D/4D measurements (2D/4D is lower in males than in females); (2) a low 2D/4D is observed across races and countries; (3) 2D/4D is closely related to fetal growth, sperm count, family size, myocardial infarction, and breast cancer; and (4) 2D/4D is related to sexual differentiation, the production of sex hormones in the fetal stage, and disease programming in the fetal stage. In addition, there is an inverse correlation between 2D/4D and testosterone concentration at the fetal stage, and 2D/4D correlates with the CAG repeat number in the androgen receptor gene [15].

A study of female twins conducted by Paul et al. [16] showed that the concordance rate of 2D/4D is higher in monozygotic twins than in dizygotic twins, that the heritability of 2D/4D is approximately 66%, and that the genetic contribution to 2D/4D in females may be more influential than the effects of prenatal environmental factors. Although it is uncertain whether these findings differ significantly between males and females in the absence of any report for males, it seems possible that 2D/4D is affected by both hereditary and secondary perinatal environmental factors.

One study showed that the mean 2D/4D did not change with gestational age from the 9th week to the 40th week [17]. In addition, there was a small increase in 2D/4D with age, which was lowest in the right hand [18]. This study indicates that 2D/4D is probably established in the uterus and that this ratio remains almost constant until adult life.

Because 2D/4D, an easily measurable physical feature, is already determined in utero and remains constant until adult life, it can be used regardless of age differences among subjects and is universal; moreover, its measurement is noninvasive. Therefore, 2D/4D is an excellent parameter for evaluating a group of autistic patients.

In genomic scans of families having more than one member with autism, the susceptibility loci for autism were investigated, and identified; these included 2q21–q33 [3,4]. In the candidate genes located here, the NRP2 gene is reported as one of the genes related to autism [19]. In addition, specific polymorphism has been found in distal-less 2 (DLX2) and cAMP guanine nucleotide exchange factor II (cAMP-GEFII) in a few cases of autism [20]. On the other hand, no significant correlation has been reported between autism and distal-less 1 (DLX1) [20,21] and DLX2 [20]. With regard to *HOXD* genes, Bacchlli et al. reported that there is no relationship between *HOXD1* and autism [20]. There has been no report on *HOXD11*, *HOXD12* or *HOXD13* to date.

It seems that these genes may be found to be significant in the development of autism when cases as a study subject have been carefully chosen and classified by the specific characteristics of presenting behavior or phenotypic clinical presentations.

The present study has limitations because it is a case-control study, rather than a family study, with a small number of subjects enrolled. However, in this study,

Please cite this article in press as: Sugie Y et al. Study of *HOXD* genes in autism particularly regarding the ratio of second to fourth digit length. Brain Dev (2009), doi:10.1016/j.braindev.2009.05.005

HOXD11 SNP -112G/-112T heterozygosity was specifically observed in autism patients with low 2D/4D. On the basis of this result, we expect that the relationships between autism and the *HOXD* genes or other candidate genes located in 2q will be clarified by studying a larger population with low 2D/4D, that is, by studying patients heterozygous for -112G/-112T in the *HOXD11* promoter.

References

[1] International Molecular Genetic Study of Autism Consortium. A full genome screen for autism with evidence for linkage to a region on chromosome 7q. Hum Mol Genet 1998;7:571–8.

[2] Yang MS, Gill M. A review of gene linkage, association and expression studies in autism and an assessment of convergent evidence. Int J Dev Neurosci 2007;25:69–85.

[3] Buxbaum JD, Silverman JM, Smith CJ, Kilifarski M, Reichert J, Hollander E, et al. Evidence for a susceptibility gene for autism on chromosome 2 and for genetic heterogeneity. Am J Hum Genet 2001;68:1514–20.

[4] Shao Y, Wolpert CM, Raiford KL, Menold MM, Donnelly SL, Ravan SA, et al. Genomic screen and follow-up analysis for autistic disorder. Am J Med Genet 2002;114:99–105.

[5] Alarcón M, Cantor RM, Liu J, Gilliam Cthe Autism Genetic Resource Exchange Consortium, Geschwind H. Evidence for a language quantitative trait locus on chromosome 7q in multiplex autism families. Am J Med Genet 2002;70:60–71.

[6] Manning JT, Baron-Cohen S, Wheelwright S, Sanders G. The 2nd to 4th digit ratio and autism. Dev Med Child Neurol 2001;43:160–4.

[7] Osawa J, Sugie H, Fukuda T, Ito M, Sugie Y, Ohzeki T. Evaluation of the 2nd to 4th digit ratio in the patients with autism. No To Hattatsu (Tokyo) 2005;37:424–5, [in Japanese].

[8] Zákány J, Fromental-Ramain C, Warot X, Duboule D. Regulation of number and size of digits by posterior Hox genes: a dose-dependent mechanism with potential evolutionary implications. Proc Natl Acad Sci USA 1997;94:13695–700.

[9] Kuroiwa A. The role of homeobox genes on cartilage pattern formation. Jikken Igaku 2002;17:2441–8, [in Japanese].

[10] American Psychiatric Association. Diagnostic and statistical manual of mental disorders. 4th ed. Washington, DC: American Psychiatric Association; 1994.

[11] Alarcón M, Yonan AL, Gilliam TC, Cantor RM, Geschwind DH. Quantitative genome scan and Ordered-Subsets Analysis of autism endophenotypes support language QTLs. Mol Psychiatry 2005;10:747–57.

[12] Freitag CM. The genetics of autistic disorders and its clinical relevance: a review of the literature. Mol Psychiatry 2007;12:2–22.

[13] Alarcón M, Abrahams BS, Stone JL, Duvall JA, Perederiy JV, Bomar JM, et al. Linkage, association, and gene-expression analyses identify *CNTNAP2* as an autism-susceptibility gene. Am J Hum Genet 2008;82:150–9.

[14] Manning JT, Churchill AJ, Peters M. The effects of sex, ethnicity, and sexual orientation on self-measured digit ratio (2D:4D). Arch Sex Behav 2007;36:223–33.

[15] Manning JT, Bundred PE, Flanagan BF. The ratio of 2nd to 4th digit length: a proxy for transactivation activity of the androgen receptor gene? Med Hypotheses 2002;59:334–6.

[16] Paul SN, Kato BS, Cherkas LF, Andrew T, Spector TD. Heritability of the second to fourth digit ratio (2d:4d): a twin study. Twin Res Hum Genet 2006;9:215–9.

[17] Malas MA, Dogan S, Evcil EH, Desdicioglu K. Fetal development of the hand, digits and digit ratio (2D:4D). Early Hum Dev 2006;82:469–75.

[18] Trivers R, Manning J, Jacobson AA. Longitudinal study of digit ratio (2D:4D) and other finger ratios in Jamaican children. Horm Behav 2006;49:150–6.

[19] Wu S, Yue W, Jia M, Ruan Y, Lu T, Gong X, et al. Association of the neuropilin-2 (NRP2) gene polymorphisms with autism in Chinese Han population. Am J Med Genet B Neuropsychiatr Genet 2007;144B:492–5.

[20] Bacchelli E, Blasi F, Biondolillo M, Lamb JA, Bonora E, Barnby G, et al. Screening of nine candidate genes for autism on chromosome 2q reveals rare nonsynonymous variants in the cAMP-GEFII gene. Mol Psychiatry 2003;8:916–24.

[21] Hamilton SP, Woo JM, Carlson EJ, Ghanem N, Ekker M, Rubenstein JL. Analysis of four DLX homeobox genes in autistic probands. BMC Genet 2005;6:52.

Please cite this article in press as: Sugie Y et al. Study of *HOXD* genes in autism particularly regarding the ratio of second to fourth digit length. Brain Dev (2009), doi:10.1016/j.braindev.2009.05.005

Ther Adv Neurol Disord
(2010) 3(2) 127–135
DOI: 10.1177/1756285609359546

A preclinical trial of sialic acid metabolites on distal myopathy with rimmed vacuoles/ hereditary inclusion body myopathy, a sugar-deficient myopathy: a review

May Christine V. Malicdan, Satoru Noguchi and Ichizo Nishino

***Abstract*:** Distal myopathy with rimmed vacuoles (DMRV), also called hereditary inclusion body myopathy (hIBM), is a moderately progressive hereditary muscle disorder affecting young adults. DMRV/hIBM is characterized clinically by muscle atrophy and weakness initially involving the distal muscles, and pathologically by the presence of small angular fibers, formation of rimmed vacuoles and deposition of various proteins in the muscle fibers. This disease is known to be caused by mutations in the UDP-*N*-acetylglucosamine 2-epimerase/*N*-acetylmannosamine kinase gene, which encodes the essential enzyme in sialic acid biosynthesis, leading to a reduction of sialic acid levels in the serum and skeletal muscles of affected patients. As it is a metabolic disease, metabolite supplementation is theoretically one of the therapeutic options. In this review, recent animal models for DMRV/hIBM are briefly characterized followed by a focus on the administration of sialic acid metabolites as a reliable therapeutic option to DMRV/hIBM with the following points highlighted: the property of compounds, the pharmacokinetic metabolism *in vivo*, and the therapeutic effects on the DMRV/hIBM mouse model.

***Keywords*:** sialic acid, GNE, muscular dystrophy, amyloid, therapy

Introduction

Distal myopathy with rimmed vacuoles (DMRV) or hereditary inclusion body myopathy (hIBM) is an autosomal recessive debilitating disorder affecting young adults with the age of onset ranging from 15 years to the late 30s [Nonaka *et al.* 2005; Nishino *et al.* 2002], and is due to mutations in the UDP-*N*-acetylglucosamine 2-epimerase/*N*-acetylmannosamine kinase (*GNE*) gene [Eisenberg *et al.* 2001]. The disease is characterized clinically by preferential involvement of the tibialis anterior and hamstring muscles and relative sparing of the quadriceps [Nishino *et al.* 2005; Nonaka *et al.* 2005; Argov and Yarom, 1984]. The course of the disease is gradually progressive, whereby patients usually become wheelchair-bound around 12 years after the onset of the disease. Findings in skeletal muscle biopsy include the presence of rimmed vacuoles, which are seen as clusters of autophagic vacuoles on electron microscopy, scattered atrophic fibers, and muscle fiber degeneration.

Despite the identification of the causative gene, the treatment for DMRV/hIBM has remained elusive as the pathomechanism of this disease has not been fully clarified. In addition, the lack of an appropriate model for understanding the disease and evaluating potential treatment options has contributed to the lag in development of a cure. In general, several strategies exist for the treatment of hereditary muscle disorders, such as gene therapy, cell therapy, and a pharmacological approach. Among these options, pharmacological treatment has been the most widely applied strategy to many muscular dystrophies and myopathies, as both the drug and study protocol can be flexibly designed based on the cause, pathogenesis, and symptoms of the disease.

This review focuses on a treatment option based on the notion of decreased sialic acid production in muscle cells owing to mutations in the *GNE* gene. Based on our recent findings on the preclinical trial of sialic acid metabolites to the

Correspondence to:
Ichizo Nishino
Department of Neuromuscular Research, National Institute of Neuroscience, National Center of Neurology and Psychiatry, Kodaira, Tokyo, Japan
nishino@ncnp.go.jp

May Christine V. Malicdan, Satoru Noguchi
Department of Neuromuscular Research, National Institute of Neuroscience, National Center of Neurology and Psychiatry, Kodaira, Tokyo, Japan

DMRV/hIBM mouse model, we review the properties of potential compounds taking into account the application *in vivo* of these compounds to mice. Likewise, we also discuss the phenotype of the mouse model and its response to therapy in order to clarify the reliability of sialic acid supplementation for DMRV/hIBM therapy in the future.

Distal myopathy with rimmed vacuoles/hereditary inclusion body myopathy animal models

Several strategies based on genetic technology by manipulating the *GNE* gene have been attempted to generate animal models for DMRV/hIBM. Simple knock-out mice represent embryonic lethality by 9.5 dpc to suggest the importance of sialic acid in early embryogenesis [Schwarzkopf *et al.* 2002]. The same concept of the importance of sialic acid was recently demonstrated in knock-in mice carrying the p.M712T mutation, which is the most common *GNE* mutation among Jewish patients. The p.M712T mice showed a renal phenotype so severe that most homozygous mice could not survive beyond 3 days after birth (P3) [Galeano *et al.* 2007]. This renal phenotype is apparently caused by an anomaly in the morphogenesis of glomerular tissues due to the remarkable reduction in sialylation of podocalyxin, a major sialylated component of podocytes. In the M712T mice that were able to survive beyond P3, however, a phenotype pointing to skeletal muscle weakness or abnormalities in muscle pathology was not found. This result may suggest that the essential requirement of *GNE* activities for a certain level of sialic acid production is different between human and mice; in other words, the need for sialic acid at least during development might be higher in mice as compared with humans.

Our group adopted a different strategy to generate $Gne^{-/-}$h*GNE*D176VTg, a mouse model for DMRV/hIBM. This model harbored a transgene of p.D176V mutated human *GNE* cDNA but is knocked-out of endogenous Gne, creating a scenario in which only mutated GNE proteins are highly expressed and the endogenous *GNE* gene was disrupted [Malicdan *et al.* 2007a,b]. These mice were born at an almost Mendelian rate with a normal appearance (Figure 1(a)). As expected, blood and several organs including skeletal muscle exhibited hyposialylation. With age, these mice reproduced several myopathic phenotypes seen in the muscles of human DMRV/hIBM patients (Figure 1(b)–(d)). After 20 weeks of age, the DMRV/hIBM mice showed physiologic muscle weakness, seen as impaired motor performance of the mouse and reduced force generation of the skeletal muscle [Malicdan *et al.* 2008]. This reduction of the force can be attributed to muscle atrophy, as specific twitch and tetanic forces per cross-section area are maintained at normal values. The reduction in gross size of the skeletal muscle is accompanied by an increase in the number of small angular fibers on muscle cross-sections (Figure 1(c), white arrows). Serum creatine kinase is moderately elevated at this age. After 30 weeks of age, specific force generation in the gastrocnemius and tibialis anterior muscles was notably reduced, while in muscle pathology variation in muscle fiber size was more remarkable, and intracellular deposition of amyloid and other various proteins was noted in the gastrocnemius muscle. After 40 weeks, the muscle force generation increasingly worsened, as reflected by increased twitch/tetanic ratio, which could likely be due to the appearance of the characteristic rimmed vacuole (Figure 1(c), red arrows) and accumulation of autophagic vacuoles [Malicdan *et al.* 2007a,b] that can impair the contractile system of the muscle. With these results, the $GNE^{-/-}$hGNED176VTg mouse is the only existing pathogenic model for DMRV/hIBM at the moment.

Potential compounds for therapy of distal myopathy with rimmed vacuoles/hereditary inclusion body myopathy

DMRV/hIBM is caused by mutations in the *GNE* gene, most of which are missense in the *GNE* gene. *GNE* encodes a critical enzyme, uridine diphosphate-N-acetylglucosamine (UDP-GlcNAc) 2-epimerase/N-acetylmannosamine (ManNAc) kinase, for the biosynthesis of sialic acid in higher vertebrates including mammals (Figure 2, left panel). This enzyme catalyzes two steps in the sialic acid biosynthesis pathway: the epimerization of UDP-GlcNAc to ManNAc and the phosphorylation of ManNAc, the product of which is the substrate used to make sialic acid. Sialic acid production is determined by a negative feedback effect of the produced sialic acid on this UDP-GlcNAc 2-epimerase/ManNAc kinase (GNE protein) step. The sialic acid product, cytidine monophosphate-neuraminate (CMP-NeuAc), binds the allosteric site of the GNE protein, inhibiting UDP-GlcNAc 2-epimerase activity. In principle, *GNE*

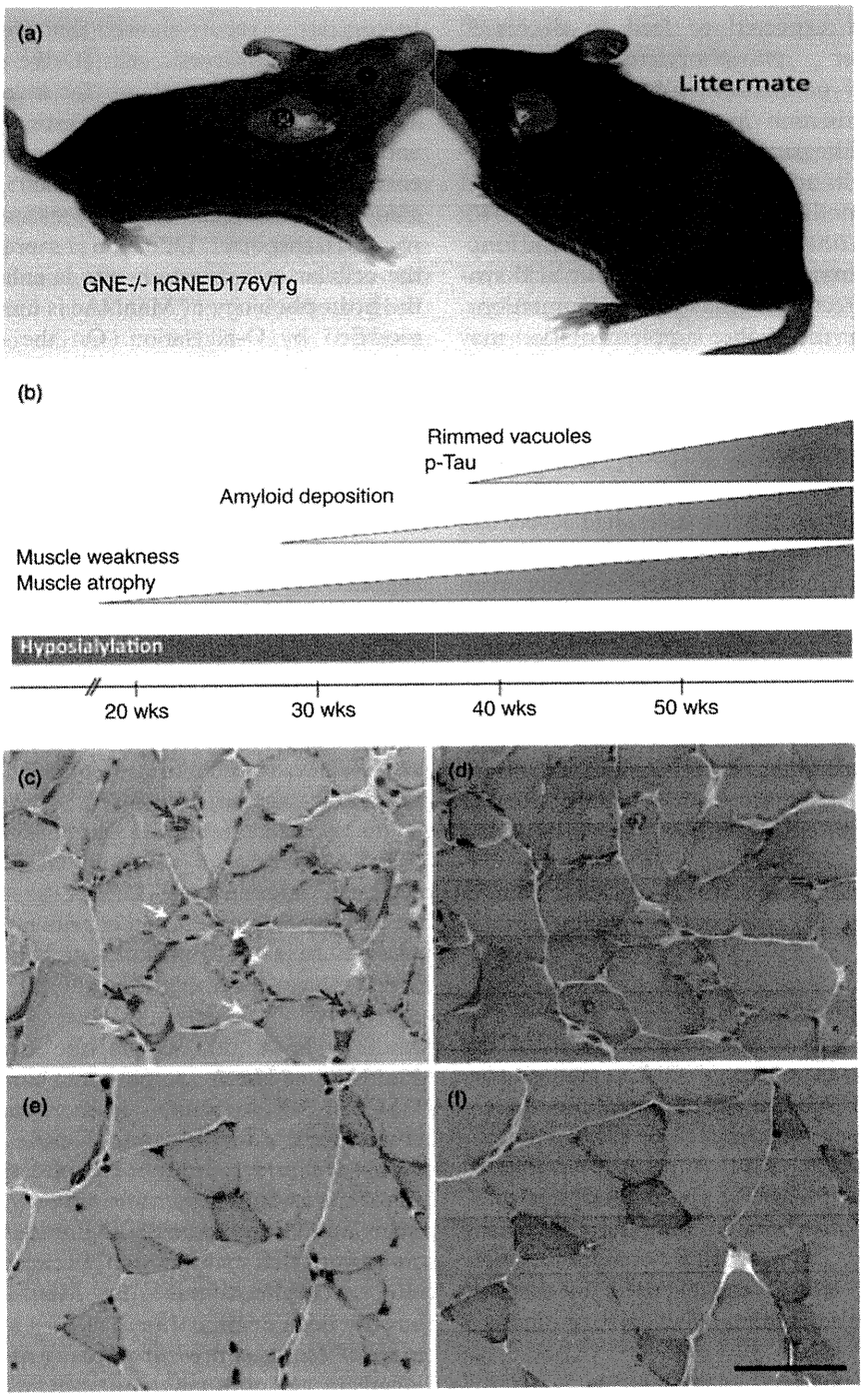

Figure 1. Overall phenotype of the distal myopathy with rimmed vacuoles (DMRV)/hereditary inclusion body myopathy (hIBM) mouse. (a) At birth, DMRV/hIBM mice appear normal, although slightly smaller than control littermates. (b) The onset of changes in muscle pathology are increasingly noted with age. Note that hyposialylation of serum and other organs is observed from birth. Typical fibers with rimmed vacuoles (red arrows) and small atrophic fibers (white arrows) are seen on hematoxylin and eosin (H&E) (c) and modified Gomori trichrome (mGT) (d). (e) H&E and (f) mGT-stained sections of muscle from age-matched control littermates. The characteristic features of DMRV/hIBM in muscle pathology are not seen in littermates. 187 × 295 mm (400 × 400 dpi).